

Effect of the tetrahedral distortion on the electronic properties of iron-pnictides

M.J. Calderón,^{1,*} B. Valenzuela,^{1,2,†} and E. Bascones^{1,‡}

¹*Instituto de Ciencia de Materiales de Madrid, ICMM-CSIC, Cantoblanco, E-28049 Madrid (Spain)*

²*Departamento de la Materia Condensada, Universidad Autónoma de Madrid, Cantoblanco, E-28049 Madrid (Spain)*

(Dated: February 10, 2022)

We study the dependence of the electronic structure of iron pnictides on the angle formed by the arsenic-iron bonds. Within a Slater-Koster tight binding model which captures the correct symmetry properties of the bands, we show that the density of states and the band structure are sensitive to the distortion of the tetrahedral environment of the iron atoms. This sensitivity is extremely strong in a two-orbital (d_{xz} , d_{yz}) model due to the formation of a flat band around the Fermi level. Inclusion of the d_{xy} orbital destroys the flat band while keeping a considerable angle dependence in the band structure.

PACS numbers: 75.10.Jm, 75.10.Lp, 75.30.Ds

The recent discovery of high temperature superconductivity in iron arsenides¹ has triggered off intense research in the condensed matter community. The characteristic building blocks of these materials are FeAs layers with each Fe atom surrounded by four arsenic atoms in a distorted tetrahedral geometry. Fe atoms form a square lattice, while As atoms located at the center of each square are displaced above and below from the Fe-plane in a checkerboard form (see Fig. 1). Undoped compounds are compensated semimetals which undergo a structural and a magnetic transition.^{2,3} Upon chemical doping, the structural distortion and magnetic order disappear and superconductivity emerges. Superconductivity has been reported so far in three families: rare-earth oxyarsenides¹ ReFeAsO , also denoted 1111 systems, with Re a lanthanide atom, TFe_2As_2 with T an alkaline earth metal and two FeAs planes per unit cell,⁴ called 122, and LiFeAs .⁵ Iron arsenides can be considered part of a larger family, the iron pnictides, with As substituted by an isovalent pnictogen element, as P.⁶

Hopping between Fe atoms via As is expected to give the dominant contribution to the kinetic energy⁷ and to the exchange interaction.⁸ Therefore some dependence of the electronic properties on the angles formed by the Fe-As bonds, i.e on the distortion of the As tetrahedron, is expected. This dependence is of crucial importance for both weak coupling models,^{9,10,11} based on nesting properties, and strong coupling models,⁸ based on superexchange interaction, aimed to explain the properties of these systems. For each family of iron-pnictides, the As tetrahedron presents different distortions. It is almost regular³ in the 122 family with the four As-Fe-As angles close to the ideal value 109.47° , while it is elongated in LiFeAs ,⁵ with As atoms further from the Fe-plane than in the regular tetrahedron (the $\text{As}^{\text{top}}\text{-Fe-As}^{\text{top}}$ angle equals 102.8°). Here As^{top} refer to an As atom placed above the Fe plane. In the 1111 family the tetrahedron is squashed and the $\text{As}^{\text{top}}\text{-Fe-As}^{\text{top}}$ or $\text{P}^{\text{top}}\text{-Fe-P}^{\text{top}}$ angle depends on specific composition, being equal to 113.7° in LaFeAsO ¹ and 120.6° in LaFePO .⁶ Differences in the electronic properties of these compounds have been attributed to the different distortion of the tetrahedra.¹² The As-Fe-

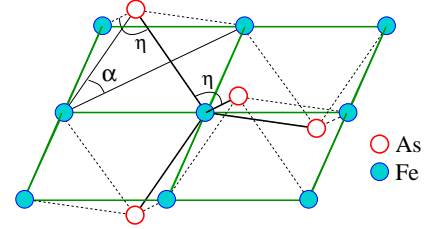


FIG. 1: Lattice structure of the FeAs layers with each Fe atom surrounded by four As atoms in a distorted tetrahedral geometry. The Fe atoms form a square lattice. At the center of each square, above and below in a checkerboard form, lie the As atoms. α , the angle formed by the Fe-As bond and the Fe-plane, is related to the $\text{As}^{\text{top}}\text{-Fe-As}^{\text{top}}$ (or Fe-As-Fe , with the Fe atoms being next nearest neighbors) angle η as $2\alpha = 180^\circ - \eta$. For instance, for a regular tetrahedron $\eta = 109.47^\circ$ and $\alpha = 35.26^\circ$.

As angle is also sensitive to doping^{13,14,15,16,17} and can be deeply modified under pressure.¹⁸ An example of the latter is the collapsed tetragonal phase found in CaFe_2As_2 under pressure.¹⁸ In Refs. 13 and 14 a possible correlation between the superconducting critical temperature and the As-Fe-As angle has been suggested with deviations within a family from the regular tetrahedron being detrimental for superconductivity. In $\text{Ba}_{1-x}\text{K}_x\text{Fe}_2\text{As}_2$ at optimal doping the tetrahedron changes from squashed (in underdoped) to elongated (in overdoped).¹⁷ It has been argued^{13,14} that there is a correlation between stronger interaction and higher critical temperature in iron pnictides due to a narrower bandwidth for the regular tetrahedron. This argument seems to be supported by the lower critical temperatures and lack of structural distortion and magnetism in LiFeAs and LaFePO . An unusually large sensitivity of the iron moment¹⁹ and the band structure^{10,20,21} to the separation of the As atoms with respect to the plane has been also found in Density Functional theory calculations.

In this paper we analyze the angle dependence of the band structure within a tight-binding model in which hopping between Fe atoms is assumed to be mediated

by As and its magnitude is calculated within the Slater Koster framework.²² We show that the two-orbital model which only includes d_{xz} and d_{yz} is extremely sensitive to changes in the angle formed by the As-Fe bonds. Such a sensitivity originates in the appearance of flat bands in the $(0,0) - (\pm\pi,0)$ and $(0,0) - (0,\pm\pi)$ directions for the regular tetrahedron case. The corresponding peak in the density of states is found at the Fermi level at half filling. The flat bands disappear when the tetrahedron is distorted. Within the present model this result is independent of any fitting parameter. Inclusion of the d_{xy} orbital modifies this picture but maintains the dependence of the density of states and band structure on the angle.

Two-orbital model. We construct a tight binding model to describe the band structure of the FeAs layers around the Fermi level in the tetragonal phase. We describe the distortion of the tetrahedron in terms of the angle α formed by the Fe-As bond direction with the Fe-plane, see Fig. 1. The advantage of using this angle, instead of the more common Fe-As-Fe or As-Fe-As ones, is that it is uniquely defined. On the contrary, there are two different Fe-As-Fe angles (depending on whether the Fe atoms are nearest or next-nearest neighbors) and, for non-regular tetrahedra there are also two different As-Fe-As angles (between top As and between top and down As). The correspondence between α and the Fe-As-Fe or As-Fe-As angles is straightforward (see figure caption of Fig. 1).

According to first principles calculations several bands cross the Fermi level and the density of states (DOS) at the Fermi level is dominated by Fe-d orbitals with little weight of pnictogen p-orbitals.^{7,20,23} We work in the Fe-square lattice and take x and y axes along the Fe-Fe bonds. Only the Fe-orbitals are included in the tight binding. As atoms only enter in the model indirectly via the Fe-Fe hopping amplitudes. Under these assumptions the Hamiltonian is given by:

$$\begin{aligned}
H = & \sum_{i,j,\beta,\gamma,\sigma} (t_{\beta,\gamma}^x c_{i,j,\beta,\sigma}^\dagger c_{i+1,j,\gamma,\sigma} + t_{\beta,\gamma}^y c_{i,j,\beta,\sigma}^\dagger c_{i,j+1,\gamma,\sigma} \\
& + t'_{\beta,\gamma} c_{i,j,\beta,\sigma}^\dagger c_{i+1,j+1,\gamma,\sigma} + t''_{\beta,\gamma} c_{i,j,\beta,\sigma}^\dagger c_{i+1,j-1,\gamma,\sigma} \\
& + h.c.) + \sum_{i,j,\beta,\sigma} \epsilon_\beta c_{i,j,\beta,\sigma}^\dagger c_{i,j,\beta,\sigma} - \mu
\end{aligned} \quad (1)$$

Here i, j and σ label the sites in the 2D lattice and the spin respectively, while β, γ refer to the Fe-d orbitals included in the tight binding. ϵ is the on-site energy, and μ is the chemical potential. We first restrict ourselves to two degenerate d_{xz} and d_{yz} orbitals, as in other minimum models recently discussed.^{24,25} Due to the degeneracy of d_{xz} and d_{yz} orbitals the onsite energies $\epsilon_{xz} = \epsilon_{yz}$ only shift the bottom of the bands and for simplicity we take them equal to zero. The hopping amplitudes t are calculated from orbital overlap integrals within the Slater-Koster framework,²² which captures the correct symmetry properties of the energy bands. Direct Fe-Fe hopping is neglected, i.e. we assume that all hopping takes place via As atoms. Neglecting the energy splitting between As

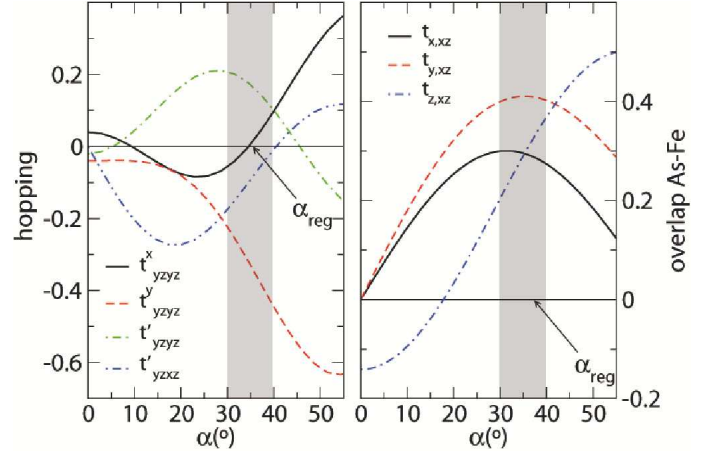


FIG. 2: Angle dependence of the Fe-Fe hopping parameters (left) and Fe-As overlap integrals (right) which enter in the two-orbital model. Fe-As overlap integrals and Fe-Fe hopping parameters are in units of pd_σ and $pd_\sigma^2/(\epsilon_d - \epsilon_p)$ respectively. $pd_\pi = -0.2$. Shaded areas correspond to the experimentally relevant angles.

$p_{x,y}$ and p_z orbitals and to second order in perturbation theory:

$$t_{xz,xz}^x = 2 [(t_{x,xz})^2 - (t_{y,xz})^2 - (t_{z,xz})^2] / (\epsilon_d - \epsilon_p) \quad (2)$$

$$t_{xz,xz}^y = 2 [(t_{x,xz})^2 - (t_{y,xz})^2 + (t_{z,xz})^2] / (\epsilon_d - \epsilon_p) \quad (3)$$

and $t_{yz,yz}^x = t_{xz,xz}^y$, $t_{yz,yz}^y = t_{xz,xz}^x$. Hopping to nearest neighbors between xz and yz vanishes. Next nearest neighbor hopping amplitudes satisfy $t''_{xz,yz} = -t'_{xz,yz}$, $t''_{xz,xz} = t'_{xz,xz}$, $t''_{yz,yz} = t'_{yz,yz}$ and $t'_{yz,yz} = t'_{xz,xz}$ with

$$t'_{xz,xz} = [(t_{x,xz})^2 + (t_{y,xz})^2 - (t_{z,xz})^2] / (\epsilon_d - \epsilon_p) \quad (4)$$

$$t'_{xz,yz} = [-t_{x,xz}t_{x,yz} - t_{y,xz}t_{y,yz} - t_{z,xz}t_{z,yz}] / (\epsilon_d - \epsilon_p) \quad (5)$$

with ϵ_p and ϵ_d the on-site energy of the pnictogen-p and Fe-d orbital, and $t_{\delta,\beta}$, with $\delta = x, y, z$ and $\beta = xz, yz$, the overlap between As- p_δ and Fe- d_β orbitals. These expressions take into account that two As atoms mediate the hopping between nearest neighbors, while only one As atom is involved in the hopping between next nearest neighbors. Overlap between As-p orbitals and Fe-d orbitals is given in terms of two integrals, taken as disposable constants, pd_σ and pd_π , where as usual σ and π refer to the component of angular momentum around the axis.²² The sign of pd_π is taken opposite to that of pd_σ .²⁶ The angle-dependence is evident in the Fe-As overlaps:

$$t_{x,xz} = \sin \alpha \left(\frac{\sqrt{3}}{2} \cos^2 \alpha (pd_\sigma) + \sin^2 \alpha (pd_\pi) \right) \quad (6)$$

$$t_{y,xz} = \frac{1}{2} \sin \alpha \cos^2 \alpha \left(\sqrt{3}(pd_\sigma) - 2(pd_\pi) \right) \quad (7)$$

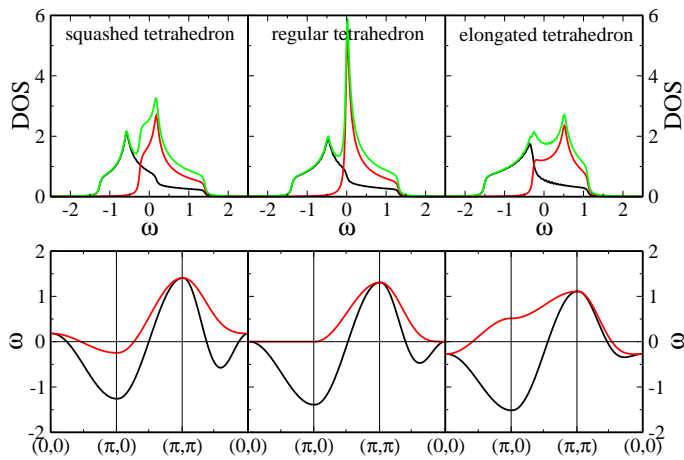


FIG. 3: Top (bottom) figures: Density of states (band structure) for the two-orbital model corresponding to the squashed (left), regular (middle) and elongated (right) tetrahedron. The corresponding angles are $\alpha = 32.71^\circ$, 35.26° and 39.13° , respectively. In the top figures the green (light) lines show the total density of states. Black and red lines give the density of states corresponding to the E^- and E^+ bands (Eq. 9) respectively. The density of states is smoothed by a lorentzian of width 0.02. Energies are in units of $pd_\sigma^2/(\epsilon_d - \epsilon_p)$.

$$t_{z,xz} = \frac{\cos \alpha}{\sqrt{2}} \left(\sqrt{3} \sin^2 \alpha (pd_\sigma) + (1 - 2 \sin^2 \alpha) (pd_\pi) \right) \quad (8)$$

and $t_{x,yz} = t_{y,xz}$, $t_{y,yz} = t_{x,xz}$, and $t_{z,xz} = t_{z,yz}$. The angle dependence of the hopping parameters which enter in Eq. (1) and of the Fe-As overlaps are shown in Fig. 2. A strong dependence is seen, specially in the Fe-Fe hopping, for the angles found experimentally (shaded area in Fig. 2). In this figure Fe-Fe hopping parameters and Fe-As overlaps are given in units of $(pd_\sigma)^2/(\epsilon_p - \epsilon_d)$ and pd_σ respectively. In these units all the hopping amplitudes and overlap integrals depend on a unique free parameter pd_π .

Diagonalization of the Hamiltonian results in two bands

$$E^\pm(\mathbf{k}) = \epsilon_+(\mathbf{k}) - \mu \pm \sqrt{\epsilon_-(\mathbf{k})^2 + \epsilon_{xy}^2(\mathbf{k})} \quad (9)$$

with

$$\epsilon_+(\mathbf{k}) = (t_{xz,xz}^x + t_{xz,xz}^y)(\cos k_x + \cos k_y) + 4t'_{xz,xz} \cos k_x \cos k_y \quad (10)$$

$$\epsilon_-(\mathbf{k}) = (t_{xz,xz}^x - t_{xz,xz}^y)(\cos k_x - \cos k_y) \quad (11)$$

$$\epsilon_{xy}(\mathbf{k}) = 4t'_{yz,xz} \sin k_x \sin k_y$$

The density of states (DOS) for a squashed ($\alpha = 32.71^\circ$), a regular ($\alpha = 35.26^\circ$) and an elongated tetrahedron ($\alpha = 39.13^\circ$), corresponding to $\text{As}^{\text{top}}\text{-Fe-As}^{\text{top}}$ angles of 114.58° , 109.47° and 101.74° respectively, and $pd_\pi = -0.2$ is plotted in Fig. 3 (top panels). In this figure the chemical potential is at $\omega = 0$, assuming half-filling.

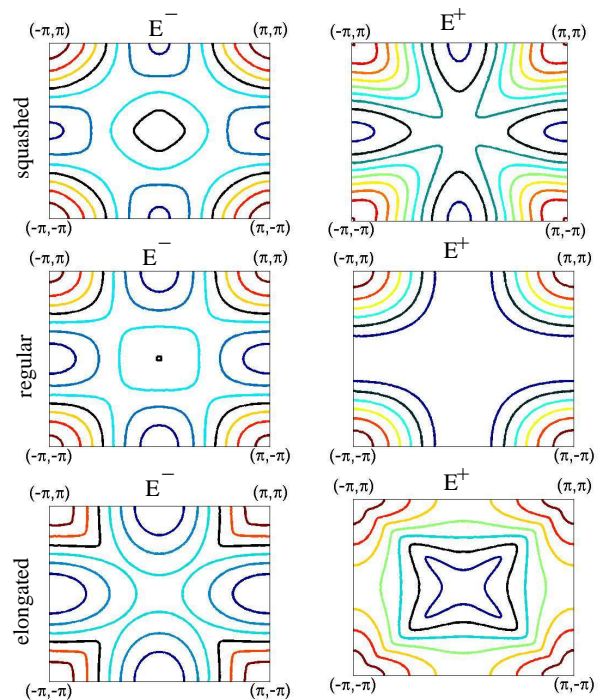


FIG. 4: Energy contour plots for the squashed (top), regular (middle) and elongated (bottom) tetrahedral geometries for the same parameters as in Fig. 3. Left figures correspond to E^- and right figures to E^+ , see Eq. 9. The Fermi surface are in black (darker lines). The topology of the Fermi surface changes with the angle.

Two peaks are observed in the DOS for the three angles. The DOS of each of the two bands E^\pm (Eq. 9) is also plotted in these figures. It can be seen that each of the peaks comes from one of the two bands. The height of the high energy peak is very strongly sensitive to α . In particular, the intensity of this peak is much higher for a regular tetrahedron. Inspection of the band structure in the lower plots of Fig. 3 reveals the existence of a flat band along $(0,0) - (\pi,0)$ in this case. By symmetry, the band is flat also along the $(0,0) - (0,\pm\pi)$ and $(0,0) - (-\pi,0)$ directions. The flat bands in the regular tetrahedron geometry ($\alpha = 35.26^\circ$) appear for any value of pd_σ and pd_π . From the expressions for the hopping amplitudes given above, for this α it can be shown that $t_{xz,xz}^x + 2t'_{xz,xz} = 0$, which cancels the k_x dependence of the band structure for $k_y = 0$ (alternatively, it cancels the k_y -dispersion for $k_x = 0$). This equality for the regular tetrahedron comes from $t_{x,xz} = t_{z,xz}$, see Eqs. (6) and (8) and right panel in Fig. 2. The topology of the energy contours and, therefore, that of the Fermi surface, is also strongly sensitive to α as shown in Fig. 4 for the same parameters used in Fig. 3.

Due to the change in the energy contour (and the Fermi surface) topology, and the very high peak in the DOS, if interactions were included, the magnetic and superconducting properties of this two-orbital model would be extremely sensitive to the angle α . This is particularly

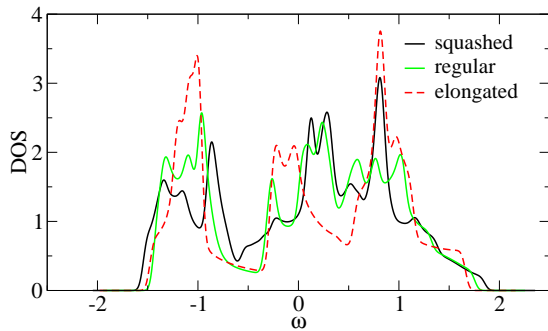


FIG. 5: Density of states for the three orbital model corresponding to the squashed, regular and elongated for the same angles as in Fig. 3, $pd_\pi = -0.2$ and $\epsilon_{xy} - \epsilon_{xz,yz} = 0.15$. The density of states is smoothed by a gaussian of width 0.03. Energies are in units of $pd_\sigma^2/(\epsilon_d - \epsilon_p)$.

evident in a picture which ascribes the magnetic transition to a spin density wave due to nesting. We show now that including a third orbital maintains some angle dependence in the electronic properties although when the hybridization with the third orbital is strong the conditions for the flat band are not fulfilled.

Three orbital model. According to LDA^{7,20,23} the d_{xy} orbital contributes to the Fermi surface and it is expected to be relevant in any description of iron pnictides.²⁷ Hamiltonian (1) can be straightforwardly generalized to include the d_{xy} or any of the e_g orbitals.²² In the case of the regular tetrahedron, including only the crystal field due to the arsenic environment, the three t_{2g} orbitals (d_{xy} , d_{yz} , and d_{xz}) are degenerate.²⁰ The inclusion of the crystal field produced by the Fe environment and/or the distortion of the tetrahedra breaks this degeneracy. As the As atom approaches the Fe-plane the d_{xy} orbital becomes higher in energy as compared to the (still degenerate) d_{xz} and d_{yz} orbitals. The level splitting $\epsilon_{xy} - \epsilon_{xz,yz}$ introduces a new parameter in the calculation. When both Fe and As crystal field effects are included $\epsilon_{xy} - \epsilon_{xz,yz}$ is slightly larger for the squashed tetrahedron than for the regular or elongated one. Expansion of hopping parameters to second order in perturbation theory also contributes to the renormalization of the on-site energies ϵ_{xy} and $\epsilon_{xz,yz}$.

For large level splittings $\epsilon_{xy} - \epsilon_{xz,yz} \gtrsim W$, with W the bandwidth of the two-orbital model, hybridization be-

tween d_{xy} and the bands E^+ and E^- of the two-orbital model is weak and the picture described above remains. However, in real materials the level splitting is expected to be smaller.²⁰ Fig. 5 shows the DOS of the three orbital model for the same geometries as in Fig. 3 and with $\epsilon_{xy} - \epsilon_{xz,yz} = 0.15$, and $pd_\pi = -0.2$. For simplicity, we neglect the angle-dependence of the level splitting. Fig. 5 reveals that a clear dependence of the DOS on the angle α still prevails within the three-orbital model. Note that the Fermi level is expected to be around the center of the band where the effect of changing the angle is very strong.²⁸ However, the origin of the dependence of the DOS on the angle α is qualitatively different to the one found in the two-orbital model: Due to the hybridization with the d_{xy} orbital the flat band that appeared in the regular tetrahedron geometry within the two-orbital model is partially destroyed in the three-band model.

In conclusion, we have analyzed the angle dependence of the band structure within a Slater-Koster based tight binding model for iron pnictides. In both two and three orbital models the density of states and therefore the Fermi surface are strongly sensitive to changes in the angle formed between the Fe-As bonds. This result is relevant for both weak coupling theories based on the nesting mechanism, which is very sensitive to the shape of the Fermi surface, and for strong coupling theories, since superexchange also depends on orbital overlaps. In the two-orbital model a flat band is formed when the As-tetrahedron is regular what results in a strong peak in the density of states. This result is robust against changes in the fitting parameters. Hybridization with a third orbital modifies this picture although the dependence on the angle remains, in particular for low energies. In our description, the bandwidth does not seem to depend very strongly on the angle, though it seems to be slightly narrower for a more elongated tetrahedron.

We thank S. Biermann, A. Cano, A. Cortijo, P. Monod, R. Roldan, A. Santander and V. Vildosola for useful conversations. E.B. thanks the hospitality of ESPCI-Paris where part of this work was done. We acknowledge funding from Ministerio de Ciencia e Innovación through Grants No. FIS2005-05478-C02-01 and MAT2006-03741, Ramón y Cajal contracts and José Castillejo program, and from Consejería de Educación de la Comunidad Autónoma de Madrid and CSIC through Grant No. CG07-CSIC/ESP-2323.

* Electronic address: calderon@icmm.csic.es

† Electronic address: belenv@icmm.csic.es

‡ Electronic address: leni@icmm.csic.es

¹ Y. Kamihara, T. Watanabe, M. Hirano, and H. Hosono, *J. Am. Chem. Soc.* **130**, 3296 (2008).

² C. de la Cruz, Q. Huang, J. W. Lynn, J. Li, W. Ratcliff, J. L. Zarestky, H. A. Mook, G. F. Chen, J. L. Luo, N. L. Wang, et al., *Nature* **453**, 899 (2008).

³ M. Rotter, M. Tegel, D. Johrendt, I. Schellenberg, W. Her-

mes, and R. Pöttgen, *Phys. Rev. B* **78**, 020503(R) (2008).

⁴ M. Rotter, M. Pangerl, M. Tegel, and D. Johrendt, *Phys. Rev. Lett.* **101**, 107006 (2008).

⁵ M. J. Pitcher, D. R. Parker, P. Adamson, S. J. C. Herkelrath, A. T. Boothroyd, and S. J. Clarke (2008), arXiv:0807.2228.

⁶ Y. Kamihara, H. Hiramatsu, M. Hirano, R. Kawamura, H. Yanagi, T. Kamiya, and H. Hosono, *J. Am. Chem. Soc.* **128**, 10013 (2006).

- ⁷ C. Cao, P. J. Hirschfeld, and H.-P. Cheng, Phys. Rev. B **77**, 220506 (2008).
- ⁸ T. Yildirim, Phys. Rev. Lett. **101**, 057010 (2008). Q. Si and E. Abrahams, Phys. Rev. Lett. **101**, 076401 (2008). T. X. Fengjie Ma, Zhong-Yi Lu (2008), arxiv:0804.3370.
- ⁹ F. Ma and Z.-Y. Lu, Phys. Rev. B **78**, 033111 (2008). J. Dong, H. Zhang, G.Xu, Z. Li, W. Hu, D. Wu, G. F. Chen, X. Dai, J. L. Luo, Z. Fang, et al., Europhys. Lett. **83**, 27006 (2008). I. Mazin, D. Singh, M. D. Johannes, and M. H Du, Phys. Rev. Lett. **101**, 057003 (2008). M. Korshunov and I. Eremin (2008), arXiv:0803.4514.
- ¹⁰ I. Mazin, M. D. Johannes, L. Boeri, and K. Koepernik, Phys. Rev. B **78**, 085104 (2008).
- ¹¹ S. Raghu, X. Qi, C.-X. Liu, D. Scalapino, and S.-C. Zhang, Phys. Rev. B **77**, 220503 (2008).
- ¹² T. McQueen, M. Regulacio, A. Williams, Q. Huang, J. W. Lynn, Y. Hor, D. West, M. Green, and R. Cava, Phys. Rev. B **78**, 024521 (2008).
- ¹³ C. Lee, A. Iyo, H. Eisaki, H. Kito, M. T. Fernandez-Diaz, T. Ito, K. Kihou, H. Matsuhata, M. Braden, and K. Yamada, J. Phys. Soc. Jpn. **77**, 083704 (2008).
- ¹⁴ J. Zhao, Q. Huang, C. de la Cruz, S. Li, J. Lynn, Y. Chen, M. Green, G. Chen, G. Li, Z. Li, et al. (2008), arXiv:0806.2528.
- ¹⁵ K.Kasperkiewicz, J.-W. G. Bos, A. Fitch, K. Prassides, and S. Margadonna (2008), arXiv:0809.1755.
- ¹⁶ Q. Huang, J. Zhao, J. W. Lynn, G. F. Chen, J. L. Luo, N. L. Wang, and P. Dai, Phys. Rev. B **78**, 054529 (2008).
- ¹⁷ M. Rotter, M. Pangerl, M. Tegel, and D. Johrendt, Angew. Chem. Int. Ed. **47**, 7949 (2008).
- ¹⁸ A. Kreyssig, M. Green, Y. Lee, G. Samolyuk, P.Zajdel, J. Lynn, S. Bud'ko, M. Torikachvili, N. Ni, S.Nandi, et al. (2008), arXiv:0807.3032.
- ¹⁹ Z. P. Yin, S. Lebègue, M. J. Han, B. P. Neal, S. Y. Savrasov, and W. E. Pickett, Phys. Rev. Lett. **101**, 047001 (2008). T. Yildirim (2008), arXiv:0807.3936.
- ²⁰ L. Boeri, O. Dolgov, and A. Golubov, Phys. Rev. Lett. **101**, 085104 (2008).
- ²¹ V. Vildosola, L.Pourovskii, R. Arita, S. Biermann, and A. Georges, Phys. Rev. B **130**, 064518 (2008).
- ²² J. C. Slater and G. F. Koster, Phys. Rev. **94**, 1498 (1954).
- ²³ S. Lebègue, Phys. Rev. B **75**, 035110 (2007). D. J. Singh and M.-H. Du, Phys. Rev. Lett. **100**, 237003 (2008). K. Haule, J. H. Shim, and G. Kotliar, Phys. Rev. Lett. **100**, 226402 (2008).
- ²⁴ M. Daghofer, A. Moreo, J. A. Riera, E. Arrigoni, and E. Dagotto (2008), arXiv:0805.0148. Y. Ran, F. Wang, H. Zhai, A. Vishwanath, and D.-H. Lee (2008), arxiv:0805.3535.
- ²⁵ X. Dai, Z. Fang, Y. Zhou, and F. chun Zhang, Phys. Rev. Lett. **101**, 057008 (2008). Z.-J. Yao, J.-X. Li, and Z. D. Wang (2008), arXiv:0804.4166. Y. Wan and Q.-H. Wang (2008), arXiv:0805.0923. T. Stanescu, V. Galitski, and S. Das Sarma (2008), arXiv:0805.2150.
- ²⁶ W. A. Harrison, *Elementary Electronic Structure* (World Scientific Publishing, 2004), page 643.
- ²⁷ P. A. Lee, and X.-G. Wen (2008), arXiv:0804.1739.
- ²⁸ A. Shorikov, M. Korotin, S. Streltsov, S. Skornyakov, D. Korotin, and V. Anisimov (2008), arXiv:0804.3283.